

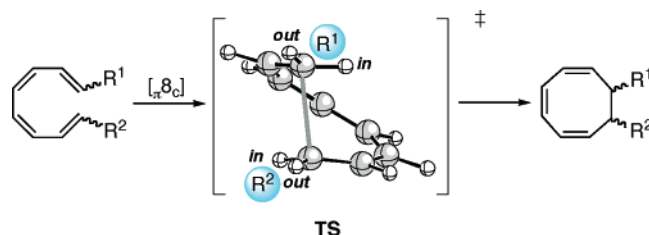
## Substituent Effects in Eight-Electron Electrocyclic Reactions

Begoña Lecea,<sup>†</sup> Ana Arrieta,<sup>‡</sup> and Fernando P. Cossío<sup>\*‡</sup>

Farmazi Fakultatea and Kimika Fakultatea, Universidad del País Vasco-Euskal Herriko Unibertsitatea, P.K. 1072, 20080 San Sebastián-Donostia, Spain

qopcomof@sq.ehu.es

Received July 2, 2004



The main features of transition structures associated with eight-electron electrocyclic reactions have been studied with Density Functional Theory. It is found that conrotatory electrocyclization reaction of (3*Z*,5*Z*)-octa-1,3,5,7-tetraenes takes place via Möbius aromatic transition structures of helical conformation. The reaction is completely periselective. In general, transition structures having outward substituents are preferred with respect to the inward transition structures, irrespective of the  $\pi$ -donor or  $\pi$ -acceptor character of the substituent. In contrast with four-electron thermal conrotatory electrocyclic reactions, there is no satisfactory correlation between the difference in energy of activation between inward and outward substituents and the Taft resonance  $\sigma_R$  parameter.

### Introduction

Electrocyclic reactions constitute an important type of pericyclic reaction, both from a theoretical<sup>1</sup> and from an experimental standpoint.<sup>2</sup> Since the formulation by Woodward and Hoffmann<sup>3</sup> of the rules that govern the stereochemistry of this kind of reaction, the concept of torquoselectivity is a major contribution to the theory of electrocyclic reactions. This term was coined by Houk et al.<sup>4</sup> for four-electron conrotatory electrocyclic reactions and distinguishes between the inward and outward disposition of the possible substituents at the transition

state (Scheme 1). Thus, the (*Z*)- and (*E*)-1,3-dienes **2** can be obtained from a given 3-substituted cyclobutene **1**, depending on the inward or outward disposition of the substituent in the corresponding transition state. According to the torquoelectronic theory, electron-withdrawing groups (EWGs) prefer to occupy the inward position, whereas electron-releasing groups (ERGs) are preferentially at the outward position.<sup>4</sup> This concept has been extended to other related systems.<sup>5</sup>

In contrast with the thermal ring opening of cyclobutenes to 1,3-dienes, the mechanism of the next conrotatory electrocyclization, namely the interconversion between (3*Z*,5*Z*)-octa-1,3,5,7-tetraenes and (*Z,Z*)-cycloocta-1,3,5-trienes, has been scarcely investigated.<sup>6–8</sup> Thus, Houk et al.<sup>6</sup> reported the transition structure

<sup>†</sup> Farmazi Fakultatea.

<sup>‡</sup> Kimika Fakultatea.

(1) (a) Woodward, R. B.; Hoffmann, R. *The Conservation of Orbital Symmetry*; Verlag Chemie International: Deerfield Beach, FL, 1970. (b) Fukui, K. *Acc. Chem. Res.* **1971**, *4*, 57.

(2) (a) Pindur, U.; Schneider, G. H. *Chem. Soc. Rev.* **1994**, 409. (b) Trost, B. M.; Fleming, I.; Paquette, L. A. *Comprehensive Organic Synthesis*; Pergamon: Oxford, UK, 1991; Vol. 5, pp 675–784. (c) Marvell, E. N. *Thermal Electrocyclic Reactions*; Academic Press: New York, 1980.

(3) Woodward, R. B.; Hoffmann, R. *J. Am. Chem. Soc.* **1965**, *87*, 395.

(4) (a) Houk, K. N. In *Strain and Its Implications in Organic Chemistry*; de Meijere, A., Blechert, S., Eds.; Kluwer Academic Publishers: Dordrecht, The Netherlands, 1989; p 25. (b) Niwayama, S.; Kallel, E. A.; Spellmeyer, D. C.; Sheu, C.; Houk, K. N. *J. Org. Chem.* **1996**, *61*, 2813. (c) Kirmse, W.; Rondan, N. G.; Houk, K. N. *J. Am. Chem. Soc.* **1984**, *106*, 7989. (d) Rondan, N. G.; Houk, K. N. *J. Am. Chem. Soc.* **1985**, *107*, 2099. (e) Dolbier, W. R., Jr.; Korionak, H.; Houk, K. N.; Sheu, C. *Acc. Chem. Res.* **1996**, *29*, 471.

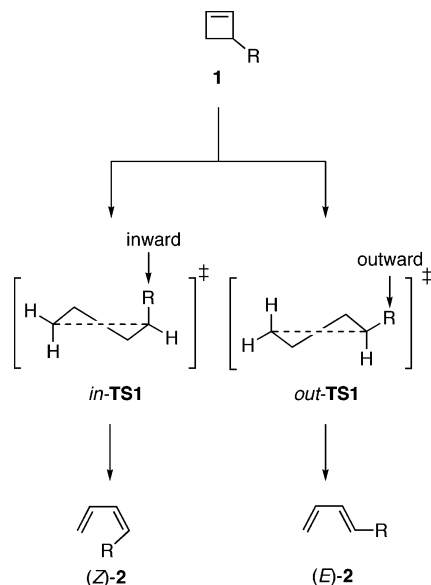
(5) See for example: (a) Cossío, F. P.; Arrieta, A.; Lecea, B.; Ugalde, J. M. *J. Am. Chem. Soc.* **1994**, *116*, 2085. (b) López, S.; Rodríguez, J.; Rey, J. G.; de Lera, A. R. *J. Am. Chem. Soc.* **1996**, *118*, 1881. (c) Evanseck, J. D.; Thomas, B. E., IV; Spellmeyer, D. C.; Houk, K. N. *J. Org. Chem.* **1995**, *60*, 7134. (d) Lecea, B.; Arrastia, I.; Arrieta, A.; Roa, G.; Lopez, X.; Arriortua, M. I.; Ugalde, J. M.; Cossío, F. P. *J. Org. Chem.* **1996**, *61*, 3070.

(6) Houk, K. N.; Li, Y.; Evanseck, J. D. *Angew. Chem., Int. Ed. Engl.* **1992**, *31*, 682.

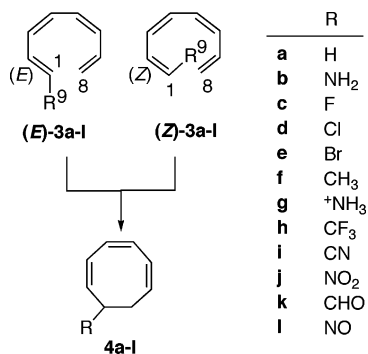
(7) Thomas, B. E., IV; Evanseck, J. D.; Houk, K. N. *J. Am. Chem. Soc.* **1993**, *115*, 4165.

(8) Jiao, H.; Schleyer, P. v. R. *J. Chem. Soc., Perkin Trans. 2* **1994**, 407.

**SCHEME 1. Stereochemistry and General Shape of Transition Structures Associated with Thermal Four-Electron Electrocyclic Reactions**



**SCHEME 2. Some Eight-Electron Conrotatory Electrocyclizations Studied in This Work**



associated with the cyclization of (*Z,Z*)-octa-1,3,5,7-tetraene **3a** (Scheme 2) and (*Z,Z,Z*)-cycloocta-1,3,5-triene **4a**, computed at the HF/6-31G\* level. These authors found a coiled conformation for this transition structure and an activation energy for the cyclization reaction of only 8 kcal/mol at the MP2/6-31G\*/HF/6-31G\* level. In a subsequent paper,<sup>7</sup> Houk et al. also reported an ab initio study (MP2/6-31G\*/HF/3-21G level) on the electrocyclic reactions of several 1-substituted 1,3,5,7-octatetraenes. In this paper, these authors concluded that, in contrast with four-electron electrocyclizations, steric effects determine the stereoselection in eight-electron conrotatory reactions thus favoring outward transition structures. On the other hand, Schleyer et al.<sup>8</sup> reported structural, energetic, and magnetic data for the same reaction. They found a very early geometry for the transition structure at the MP2(fu)/6-31G\* level, with a C–C bond forming distance ca. 0.35 Å larger than that found by Houk at the HF/6-31G\* level. These authors also found that the transition structure is aromatic according to magnetic criteria. Interestingly, they reported a big diamagnetic shielding for the inner protons of the terminal methylene groups, which was compatible with the effect induced by the diamagnetic ring current of the aromatic transition structure.

From the experimental point of view this reaction has practical relevance and, for example, plays an important role in the synthesis of polycyclic systems described by Paquette et al.<sup>9</sup> and in the biosynthesis of endiandric acids reported by Nicolaou et al.<sup>10</sup> More recently, this electrocyclization has found novel applications such as the synthesis of derivatives of (*9Z,11Z*)-vitamin A acetate and palmitate, reported by Widmer et al.<sup>11</sup> In addition, Okamura et al.<sup>12</sup> have described the synthesis of a 9,19-methanobridged analogue of 1 $\alpha$ ,25-dihydroxyvitamin D<sub>3</sub> by means of a 8 $\pi$  electrocyclization. Similarly, an interesting application of this reaction has been reported by Trauner et al.<sup>13</sup> and by Baldwin et al.<sup>14</sup> in the biomimetic synthesis of immunosuppressants SNF4435 C and D. Finally, Suffert et al.<sup>15</sup> have also applied this reaction to the expeditious synthesis of the tricyclic core of the ophiobolins and aleurodiscal.

Within this context, the aim of the present paper has been to study the conrotatory electrocyclization of mono- and polysubstituted (*E*)- and (*Z*)-octatetraenes **3** to form octatrienes **4** to evaluate the substituent effects in this reaction.

**Methods**

All the calculations reported in this paper have been performed within Density Functional Theory,<sup>16</sup> using the hybrid three-parameter functional customarily denoted as B3LYP.<sup>17</sup> The standard 6-31G\* basis set<sup>18</sup> as implemented in the GAUSSIAN 98<sup>19</sup> suite of programs has been used in all cases. Houk et al.<sup>20</sup> have shown that the B3LYP/6-31G\* level is a convenient method for the computational study of this kind of reactions in terms of computational cost and accuracy. Donor–acceptor interactions have been calculated by using the Natural Bonding Orbital method.<sup>21</sup> The energies associated with these two-electron interactions were computed by means of the second-order perturbation energy  $\Delta E_{\phi\phi^*}^{(2)}$  according to the following equation

$$\Delta E_{\phi\phi^*}^{(2)} = -n_{\phi} \frac{\langle \phi^* | \hat{F} | \phi \rangle^2}{\epsilon_{\phi^*} - \epsilon_{\phi}} \quad (1)$$

(9) (a) Paquette, L. A.; Hamme, A. T.; Kuo, L. M.; Doyon, J.; Kreuzholz, R. *J. Am. Chem. Soc.* **1997**, *119*, 1242. (b) Paquette, L. A.; Morwich, T. M. *J. Am. Chem. Soc.* **1997**, *119*, 1230. (c) Paquette, L. A. *Eur. J. Org. Chem.* **1998**, 1709. (d) Oliva, M.; Domingo, L. R.; Safont, U.-S.; Andres, J.; Castillo, R.; Moliner, V. *J. Phys. Org. Chem.* **1999**, *12*, 61.

(10) (a) Nicolaou, K. C.; Petasis, N. A. In *Strategies and Tactics in Organic Synthesis*; Lindberg, T., Ed.; Academic Press: San Diego, CA, 1984; Vol. 1, pp 155–173. (b) Nicolaou, K. C.; Petasis, N. A.; Zipkin, R. E.; Uenishi, J. *J. Am. Chem. Soc.* **1982**, *104*, 5555. (c) Nicolaou, K. C.; Petasis, N. A.; Uenishi, J.; Zipkin, R. E. *J. Am. Chem. Soc.* **1982**, *104*, 5557. (d) Nicolaou, K. C.; Petasis, N. A.; Zipkin, R. E. *J. Am. Chem. Soc.* **1982**, *104*, 5560.

(11) Vogt, P.; Schlageter, M.; Widmer, E. *Tetrahedron Lett.* **1991**, *32*, 4115.

(12) Hayashi, R.; Fernández, S.; Okamura, W. H. *Org. Lett.* **2002**, *4*, 851.

(13) Beaudry, C. M.; Trauner, D. *Org. Lett.* **2002**, *4*, 2221.

(14) Moses, J. E.; Baldwin, J. E.; Marquez, R.; Adlington, R. M.; Cowley, A. R. *Org. Lett.* **2002**, *4*, 3731.

(15) Salem, B.; Suffert, J. *Angew. Chem., Int. Ed.* **2004**, *43*, 2826.

(16) Parr, R. G.; Yang, W. *Density-Functional Theory of Atoms and Molecules*; Oxford: New York, 1989.

(17) (a) Kohn, W.; Becke, A. D.; Parr, R. G. *J. Phys. Chem.* **1996**, *100*, 12974. (b) Becke, A. D. *J. Chem. Soc.* **1993**, *98*, 5648. (c) Becke, A. D. *Phys. Rev. A* **1988**, *38*, 3098.

(18) Hehre, W. J.; Radom, L.; Schleyer, P. v. R.; Pople, J. A. *Ab Initio Molecular Orbital Theory*; Wiley: New York, 1986; pp 76–87 and references therein.

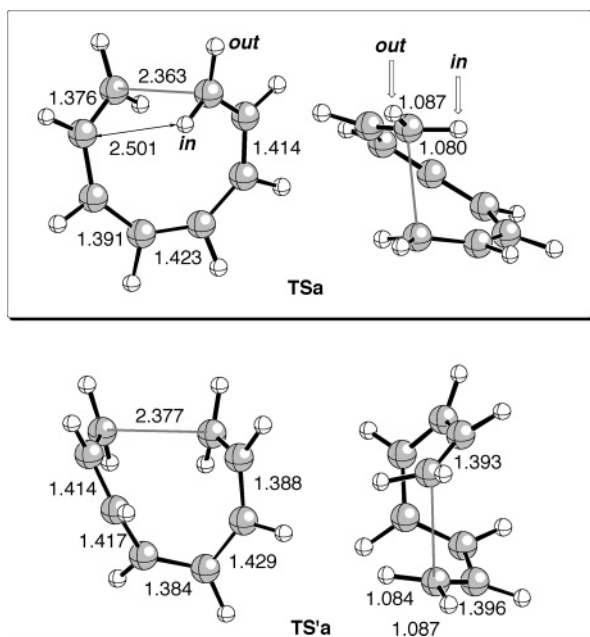


**FIGURE 1.** Fully optimized geometries (B3LYP/6-31G\* level of theory) of helix (**TSa**) and boat (**TS'a**) transition structures associated with the interconversion between (*Z,Z*)-octa-1,3,5,7-tetraene and (*Z,Z,Z*)-cycloocta-1,3,5-triene. Bond distances are given in Å. Open arrows point to the inward (*in*) and outward (*out*) positions of terminal hydrogens.

where  $\phi^*$  and  $\phi$  are the non-Lewis and Lewis localized orbitals,  $\hat{F}$  is the Fock operator,  $n_\phi$  is the occupation of the  $\phi$  localized orbital, and  $\epsilon_{\phi^*}$  and  $\epsilon_\phi$  are the respective energies.

Nucleus-independent chemical shifts (NICS) as defined by Schleyer<sup>22</sup> were computed by using the gauge invariant atomic orbital<sup>23</sup> (GIAO) approach at the GIAO-B3LYP/6-31G\*//B3LYP/6-31G\* level.

Activation energies ( $\Delta E_a$ ) and reaction energies ( $\Delta E_{\text{rxn}}$ ) have been computed at the B3LYP/6-31G\* level including zero-point vibrational energy (ZPVE) corrections, which were not scaled. These relative energies were computed starting from the all-*s*-transoid conformations of the reactants.

## Results and Discussion

First we studied the parent reaction **3a**  $\rightarrow$  **4a**. We located and characterized two possible transition structures, **TSa** and **TS'a** (Figure 1). However, only the first

(19) Frisch, M. J.; Trucks, G. W.; Schlegel, H. B.; Scuseria, G. E.; Robb, M. A.; Cheeseman, J. R.; Zakrzewski, V. G.; Montgomery, J. A., Jr.; Stratmann, R. E.; Burant, J. C.; Dapprich, S.; Millam, J. M.; Daniels, A. D.; Kudin, K. N.; Strain, M. C.; Farkas, O.; Tomasi, J.; Barone, V.; Cossi, M.; Cammi, R.; Mennucci, B.; Pomelli, C.; Adamo, C.; Clifford, S.; Ochterski, J.; Petersson, G. A.; Ayala, P. Y.; Cui, Q.; Morokuma, K.; Malick, D. K.; Rabuck, A. D.; Raghavachari, K.; Foresman, J. B.; Cioslowski, J.; Ortiz, J. V.; Stefanov, B. B.; Liu, G.; Liashenko, A.; Piskorz, P.; Komaromi, I.; Gomperts, R.; Martin, R. L.; Fox, D. J.; Keith, T.; Al-Laham, M. A.; Peng, C. Y.; Nanayakkara, A.; Gonzalez, C.; Challacombe, M.; Gill, P. M. W.; Johnson, B.; Chen, W.; Wong, M. W.; Andres, J. L.; Gonzalez, C.; Head-Gordon, M.; Replogle, E. S.; Pople, J. A. *Gaussian 98*, revision A.5; Gaussian, Inc.: Pittsburgh, PA, 1998.

(20) Guner, V.; Khuong, K. S.; Leach, A. G.; Lee, P. S.; Bartberger, M. D.; Houk, K. N. *J. Phys. Chem. A* **2003**, *107*, 11445.

(21) (a) Reed, A. E.; Curtiss, L. A.; Weinhold, F. *Chem. Rev.* **1988**, *88*, 899. (b) Reed, A. E.; Weinstock, R. B.; Weinhold, F. *J. Chem. Phys.* **1985**, *83*, 735.

(22) Schleyer, P. v. R.; Maerker, C.; Dransfeld, A.; Jiao, H.; Hommes, N. J. R. v. E. *J. Am. Chem. Soc.* **1996**, *118*, 6317.

(23) Wolinski, K.; Hilton, J. F.; Pulay, P. *J. Am. Chem. Soc.* **1990**, *112*, 8251.

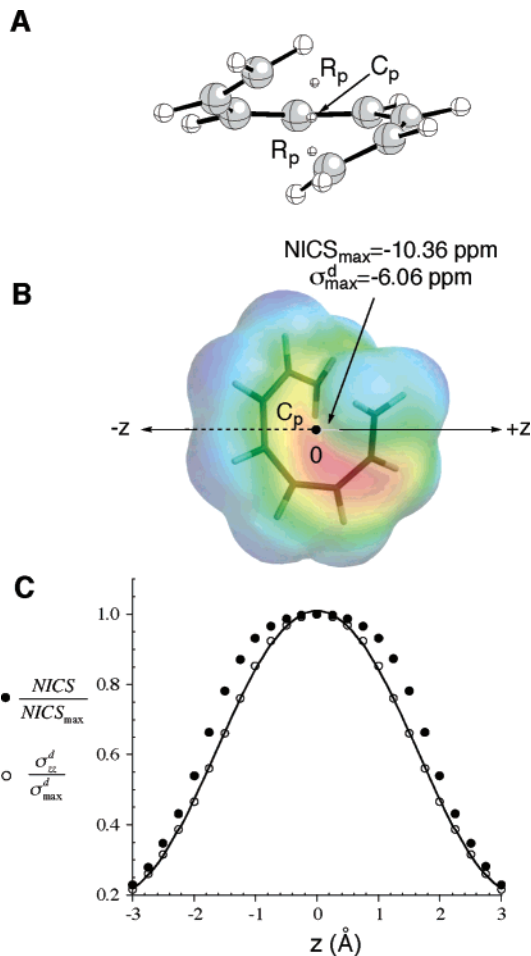


**FIGURE 2.** (A) Cage point ( $C_p$ ) and ring points ( $R_p$ ) of electron density corresponding to **TSa**. (B)  $NICS_{\text{max}}$  and  $\sigma_{\text{max}}^d$  values of **TSa** were computed at  $C_p$  (see text). The electrostatic potential has been projected on the electron density (isocontour value: 0.002 electron/bohr<sup>3</sup>). Colors range from  $-17.21$  kcal/mol (red) to  $+9.83$  kcal/mol (blue). (C):  $NICS/NICS_{\text{max}}$  vs  $z$  and  $\sigma_{zz}^d/\sigma_{\text{max}}^d$  vs  $z$  plots computed for **TSa**. The  $z$ -axis is defined in Figure 2B.

transition structure is associated with the conrotatory electrocyclization under study. **TS'a**, with a boat conformation, lies 27.4 kcal/mol above **TSa** and is associated with a disrotatory motion. According to our B3LYP/6-31G\*+ $\Delta$ ZPVE results, the **3a**  $\rightarrow$  **4a** reaction has an activation energy of 16.8 kcal/mol, a value in excellent agreement with the experimental value of 17.0 kcal/mol obtained by Goldfarb and Lindqvist.<sup>24</sup> From the geometric features of **TSa** depicted in Figure 1, it can be concluded that it is earlier than the transition structure associated with the parent four-electron reaction. Thus, the alternation of double bonds in the starting tetraene is partially preserved at **TSa**, whereas the C–C bond being formed is ca. 0.2 Å larger than that of its four-electron analogue.<sup>25</sup> Another remarkable feature of **TSa** is that its helical conformation leads to an almost perfect eclipsing between the inward position and the carbon atom contiguous to the terminal position of the starting tetraene, with an interatomic distance of ca. 2.5 Å (Figure 1). This

(24) Goldfarb, T.; Lindqvist, L. *J. Am. Chem. Soc.* **1967**, *89*, 4588.

(25) Wiest, O.; Houk, K. N.; Black, K. A.; Thomas, B. E., IV. *J. Am. Chem. Soc.* **1995**, *117*, 8594.



is a small value and it is expected that substituents occupying an inward position must exhibit a significant difference with respect to their outward congeners.

As Schleyer and Jiao mentioned in their 1994 paper,<sup>8</sup> **TSa** is interesting because of its possible Möbius aromatic character.<sup>26</sup> Therefore, to get a better understanding of the hypothetical aromatic character of **TSa**, we have calculated the NICS inside the ring being formed. In previous studies<sup>27–29</sup> we have suggested that the (3,+1) ring point ( $R_p$ ) of electron density as defined by Bader<sup>30</sup> is a convenient site to calculate the NICS of aromatic transition structures because of its high sensitivity to diamagnetic effects and its unambiguous character. However, our calculations on **TSa** led to a (3,+3) cage point ( $C_p$ ), which represents a minimum of electron density in the three directions of space (Figure 2A). This result can be understood if we take into account that the coiled geometry of **TSa** induces an appreciable electron density above and below the putative plane of the ring being formed (Figure 2A). This finding is compatible with the strong diamagnetic shielding reported by Schleyer and Jiao for the terminal inner hydrogens of this saddle point.<sup>8</sup> In addition, we have found two (3,+1) ring points ( $R_p$ ) above and below  $C_p$  (Figure 2A). Since we have also found eighteen (3,-1) bond points of electron density, associated with the carbon–hydrogen and carbon–carbon bonds (including the C–C bond being formed), the electron density analysis of **TSa** satisfies the Poincaré–Hopf relationship<sup>31</sup>

$$n - b + r - c = 1 \quad (2)$$

where  $n$  is the number of atoms of the molecule under consideration and  $b$ ,  $r$ , and  $c$  are the number of bond, ring, and cage points, respectively.

The NICS value found at the  $C_p$  of **TSa** is  $-10.36$  ppm, which indicates an aromatic character for this transition structure.<sup>32</sup> Inspection of the electrostatic potential projected on the electron density (Figure 2B) suggests that there is a strong  $\pi$ -delocalization in this transition structure. We have previously reported that for  $\pi^2$ -aromatic systems<sup>33</sup> the diamagnetic shielding at the center of the ring being formed can be approximated by two ring currents circulating above and below the average molecular plane, according to the following expression:<sup>28,29</sup>

$$\sigma_{zz}^d = -\frac{e^2\mu_0}{16\pi m_e} \left[ \left[ 1 + \left( \frac{z - R_0}{R_{av}} \right)^2 \right]^{-3/2} + \left[ 1 + \left( \frac{z + R_0}{R_{av}} \right)^2 \right]^{-3/2} \right] \quad (3)$$

(26) Minkin, V. I.; Glukhovtsev, M. N.; Simkin, B. Ya. *Aromaticity and Antiaromaticity. Electronic and Structural Aspects*; Wiley: New York, 1994; pp 104–115.

(27) Morao, I.; Lecea, B.; Cossío, F. P. *J. Org. Chem.* **1997**, *62*, 7033.

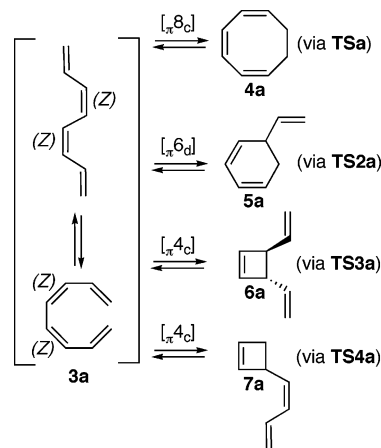
(28) Morao, I.; Cossío, F. P. *J. Org. Chem.* **1999**, *64*, 1868.

(29) Cossío, F. P.; Morao, I.; Jiao, H.; Schleyer, P. v. R. *J. Am. Chem. Soc.* **1999**, *121*, 6737.

(30) Bader, R. F. W. *Atoms in Molecules: A Quantum Theory*; Clarendon Press: Oxford, UK, 1990; pp 13–52.

(31) Collard, K.; Hall, G. C. *Int. J. Quantum Chem.* **1977**, *12*, 623. For other crowded structures involving unusual critical points of electron density see for example: Mixon, S. T.; Cioslowski, J. *J. Am. Chem. Soc.* **1991**, *113*, 6760.

### SCHEME 3. Possible Thermal Electrocyclic Reactions for (Z,Z)-Octa-1,3,5,7-tetraene **3a**



where  $\sigma_{zz}^d$  is the diamagnetic shielding constant along the  $z$  axis perpendicular to the molecular plane,  $R_0$  is the covalent radius of the atoms present in the ring under consideration, and  $R_{av}$  is the average radius of such a ring. In the present case  $R_0 = 0.750$  Å, which is the covalent radius of carbon,<sup>34</sup> and  $R_{av}$  is the average distance between  $C_p$  and the eight carbon atoms of the cycloocta-1,3,5-triene being formed, namely

$$R_{av} = \frac{1}{8} \sum_{i=1}^8 R_{C_{p,i}} = 1.853 \text{ Å} \quad (4)$$

From eq 3 it is obtained that the maximum absolute value (maximum diamagnetic shielding)  $\sigma_{max}^d$  for  $\sigma_{zz}^d$  corresponds to  $z = 0$ . Therefore, with the  $R_0$  and  $R_{av}$  values previously calculated the following value is obtained:

$$\sigma_{max}^d = -\frac{e^2\mu_0}{8\pi m_e} \left[ 1 + \left( \frac{R_0}{R_{av}} \right)^2 \right]^{-3/2} = -6.06 \text{ ppm} \quad (5)$$

According to these results, we can conclude that at least 60% of the total NICS at  $C_p$  can be assigned to ring current effects. It is also interesting to note that the variation of the NICS/NICS $_{max}^d$  values along the  $z$  axis agrees quite well with the  $\sigma_{zz}^d/\sigma_{max}^d$  vs  $z$  curve, thus indicating that even in this coiled structure the ring current model describes correctly a significant part of the diamagnetic shielding. In summary, we conclude, as Schleyer and Jiao did,<sup>8</sup> that **TSa** is a Möbius aromatic transition structure in which cyclic electron delocalization is responsible for a significant part of the diamagnetic shielding calculated for the inner regions of the ring being formed.

Aside from the  $[\pi 8c]$  mechanism above-described, at least three additional electrocyclic processes are also conceivable for (Z,Z)-octa-1,3,5,7-tetraene **3a** (Scheme 3).

(32) The computed NICS for both ring points of **TSa** is  $-9.901$  ppm, a value quite similar to that obtained for the cage point. However, we think that this latter point is more appropriate to describe the aromaticity of this transition structure because it is unique and is at the center of the cyclic structure.

(33) De Lera, A. R.; Alvarez, R.; Lecea, B.; Torrado, A.; Cossío, F. P. *Angew. Chem., Int. Ed.* **2001**, *40*, 557.

(34) Pauling, L. *The Nature of the Chemical Bond*, 3rd ed.; Cornell University Press: Ithaca, UK, 1960; p 224.

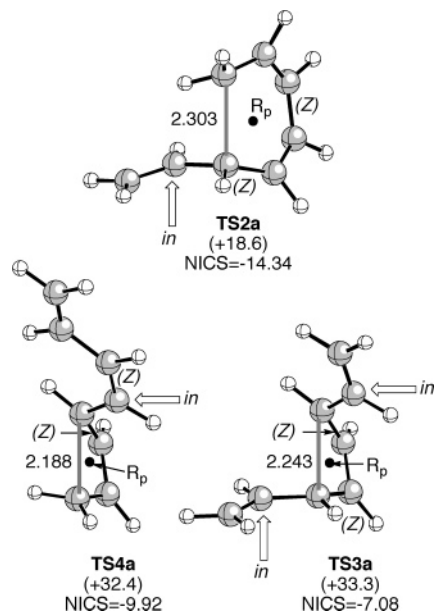


**FIGURE 3.** Geometric (B3LYP/6-31G\*), energetic (B3LYP/6-31G\*+ $\Delta$ ZPVE), and magnetic (GIAO-B3LYP/6-31G\*) features of transition structures **TS2a**, **TS3a**, and **TS4a** (see Scheme 3). Numbers in parentheses correspond to the relative energies (in kcal/mol) with respect to **TSa**.  $R_p$  denotes the ring point of electron density corresponding to each transition structure. NICS values (in ppm) have been calculated at the respective ring points. Bond distances are given in Å.

Thus, depending upon the reactive double bond array considered, one  $[\pi 6_d]$  and two  $[\pi 4_c]$  reactions can take place, to yield the products **5a**, **6a**, and **7a**, respectively, as depicted in Scheme 3. The geometric, energetic, and magnetic features of the corresponding transition structures **TS2a**, **TS3a**, and **TS4a** are reported in Figure 3. It is important to note that the geometry of the starting (*Z*)-bonds in **3a** determines the inward disposition of the substituents in these three latter transition structures (Figure 3). Since the vinyl and (*Z*)-buta-1,3-dienyl groups present in **TS2a**, **TS3a**, and **TS4a** are good  $\pi$ -donors, these inward geometries would destabilize the respective transition structures, according to the torquoelectronic theory.<sup>4</sup> As a consequence, these transition structures are associated with activation energies larger than those found for the parent  $[\pi 4_c]$  and  $[\pi 6_d]$  electrocyclizations.<sup>20</sup> Therefore, **3a** must cyclize to **4a** with complete periselectivity. In these three transition structures we obtained negative values of the NICS associated with aromatic Hückel (**TS2a**) and Möbius (**TS3a** and **TS4a**) transition structures.

We have computed the activation and reaction energies of several monosubstituted octa-1,3,5,7-tetraenes **3b–l** to yield the corresponding cyclooctatrienes **4b–l** (Scheme 2). The most relevant energetic parameters are reported in Tables 1 and 2. The chief geometric features of transition structures **TSb–g** and **TSh–l** are reported in Figures S1 and S2 of the Supporting Information, respectively.

From the data included in Figures S1 and S2, it can be concluded that the inward-substituted transition structures have larger C1...C8 bond distances than the corresponding outward-substituted analogues. In addition, saddle points **TSb–g** (Figure S1) having negative

**TABLE 1.** Activation Energies<sup>a,b</sup> ( $\Delta E_a$ , kcal/mol) and Reaction Energies<sup>a</sup> ( $\Delta E_{\text{rxn}}$ , kcal/mol) Associated with **3a–l**  $\rightarrow$  **4a–l** Reactions<sup>a,b</sup>

reactant	R	$\Delta E_a$		$\Delta E_{\text{rxn}}$	
		out	in	from ( <i>Z</i> )- <b>3</b>	from ( <i>E</i> )- <b>3</b>
<b>3a</b>	H	16.8			-5.2
<b>3b</b>	NH <sub>2</sub>	20.0	17.5	3.9	2.6
<b>3c</b>	F	16.5	18.4	-6.4	-5.8
<b>3d</b>	Cl	17.7	23.0	-5.2	-5.3
<b>3e</b>	Br	16.8	21.7	-6.9	-6.6
<b>3f</b>	CH <sub>3</sub>	18.2	20.4	-1.3	-3.0
<b>3g</b>	<sup>+</sup> NH <sub>3</sub>	17.4	11.8	-9.9	-9.9
<b>3h</b>	CF <sub>3</sub>	16.9	21.8	-5.1	-7.9
<b>3i</b>	CN	17.9	21.4	1.0	0.6
<b>3j</b>	NO <sub>2</sub>	17.2	20.3	-2.6	-5.1
<b>3k</b>	CHO	18.4	19.7	2.7	-0.5
<b>3l</b>	NO	18.7	21.8	6.3	4.8

<sup>a</sup> All energies have been computed at the B3LYP/6-31G\*+ $\Delta$ ZPVE level. <sup>b</sup> The (*E*)-**3** and (*Z*)-**3** reactants yield the corresponding products via transition structures *out*-TS and *in*-TS, respectively.

**TABLE 2.** Taft Resonance Parameters ( $\sigma_R^0$ )<sup>a</sup> and Inward–Outward Energy Differences<sup>b,c</sup> ( $\Delta E_{\text{in-out}}$ , kcal/mol) between Conrotatory Transition Structures Associated with Four- and Eight-Electron Electrocyclizations (Scheme 2)

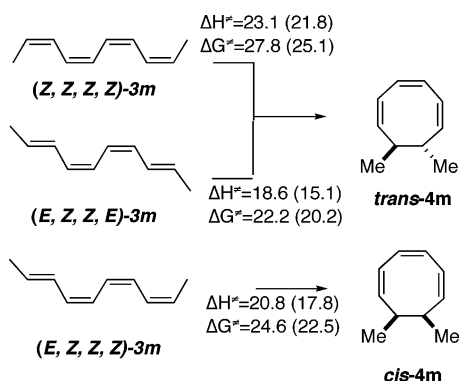
entry	R	$\sigma_R^0$	$\Delta E_{\text{in-out}}$	
			$[\pi 4_c]$	$[\pi 8_c]$
a	H	0.00	0.0	0.0
b	NH <sub>2</sub>	-0.48	14.6	-1.2
c	F	-0.32	14.8	1.4
d	Cl	-0.23	14.4	5.4
e	Br	-0.19	13.2	4.6
f	CH <sub>3</sub>	-0.11	6.2	3.9
g	<sup>+</sup> NH <sub>3</sub>	-0.04	6.6	-5.6
h	CF <sub>3</sub>	0.10	2.4	7.7
i	CN	0.13	4.5	3.8
j	NO <sub>2</sub>	0.15	6.0	5.5
k	CHO	0.26	-3.6	4.5
l	NO	0.31	-3.6	4.5

<sup>a</sup> Taft resonance parameters taken from ref 35. <sup>b</sup> Computed at the B3LYP/6-31G\*+ $\Delta$ ZPVE level of theory. <sup>c</sup>  $\Delta E_{\text{in-out}}$  values are the differences in energy between the corresponding *in* and *out* transition structures, respectively.

Taft<sup>35</sup> resonance parameters ( $\sigma_R^0$ ) (Table 2) exhibit C1...C8 bond distances similar to those calculated for transition structures **TSh–l** (Figure S2), which incorporate substituents with positive  $\sigma_R^0$  parameters. The same observation can be extended to the internuclear distances associated with R9 and C7 positions (Scheme 2). To investigate if there is some additive character between substituents, we calculated the activation and reaction energies for dimethyl derivatives **3m** to yield *cis*- or *trans*-**4m** (Scheme 4). The three possible transition structures are reported in Figure 4, together with the corresponding calculated activation and reaction energies. According to our results, the *in-in*-**TSm** is ca. 4.7 kcal/mol higher in energy than *out-out*-**TSm**, a result that can be expected from the results included in Table 2, since for R = CH<sub>3</sub>  $\Delta E_{\text{in-out}} = 3.9$  kcal/mol. Thus, *in-out*-**TSm** lies between both transition structures, its energy being 2.2 kcal/mol higher than that of *out-out*-**TSm**. Interestingly, Huisgen et

(35) Hansch, C.; Leo, A.; Taft, R. W. *Chem. Rev.* **1991**, *91*, 165.

**SCHEME 4. Electrocyclization of Different Isomers of Deca-2,4,6,8-tetraene **3m** to Yield *cis*- and *trans*-(*Z,Z,Z*)-7,8-Dimethylcycloocta-1,3,5-triene **4m**<sup>a</sup>**



<sup>a</sup> Computed (B3LYP/6-31G\*+ΔZPVE level) activation and reaction enthalpies and free energies are given in kcal/mol. The experimental values have been taken from ref 36 and are given in parentheses.

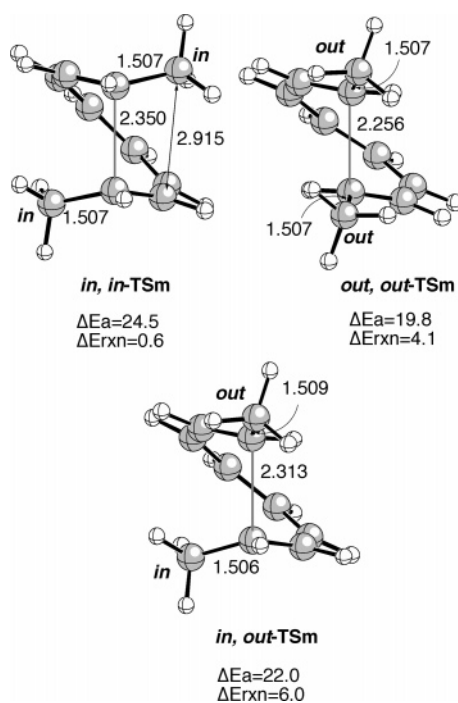


**FIGURE 4.** Chief geometric features (B3LYP/6-31G\* level of theory) of transition structures *in,in*-, *in,out*-, and *out,out*-**TSm** (see Scheme 4). Bond distances are given in Å.

al.<sup>36</sup> found that the activation parameters for the (*Z,Z,Z,Z*)-**3m** → *trans*-**4m** transformation are  $\Delta H^\ddagger = 21.8$  kcal/mol and  $\Delta S^\ddagger = -12$  emu, respectively, a result in good agreement with our computed values of  $\Delta H^\ddagger = 23.1$  kcal/mol and  $\Delta S^\ddagger = -15.7$  emu.

Houk et al.<sup>4</sup> found that there is a good correlation between the  $\sigma_R^0$  parameter and the energy difference between the corresponding inward and outward transition structures associated with [ $_{\tau}4_c$ ] reactions. In addition,

(36) (a) Huisgen, R.; Dahmem, A.; Huber, H. *Tetrahedron Lett.* **1969**, 1461. (b) Huisgen, R.; Dahmem, A.; Huber, H. *J. Am. Chem. Soc.* **1967**, 89, 7130.

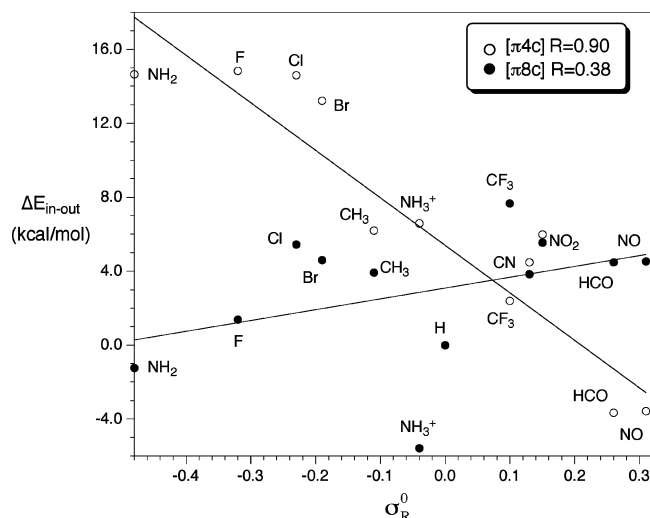


**FIGURE 5.** Differences in energy ( $\Delta E_{in-out}$ , kcal/mol, computed at the B3LYP/6-31G\*+ΔZPVE level of theory) versus Taft resonance parameters  $\sigma_R^0$  associated with *in* and *out* transition structures **Tsa–I** (black circles). Open circles show the corresponding four-electron equivalents, calculated at the same theoretical level.

tion, the same group found that in the case of [ $_{\tau}8_c$ ] electrocyclizations<sup>7</sup> there is a preference for outward transition structures in 7-substituted 1,3,5-cyclooctatrienes regardless of the electron-donating or electron-withdrawing character of the substituent. In the case of [ $_{\tau}4_c$ ] reactions, we have recalculated these differences at the B3LYP/6-31G\*+ΔZPVE level and the results are included in Table 2. In effect, at this level of theory a good correlation is obtained for four-electron conrotatory electrocyclizations, as can be seen in Figure 5. However, when we calculated the same energy differences for transition structures **Tsa–I** (Table 2), we have not obtained any significant correlation for these eight-electron conrotatory electrocyclizations, the correlation coefficient being only ca. 0.4 (Figure 5).

In agreement with Houk et al.,<sup>7</sup> our B3LYP/6-31G\*+ΔZPVE calculations show that there is a general preference for the outward transition structures associated with [ $_{\tau}8_c$ ] reactions, with the only exception being amino and ammonium groups, in which there is a preference for the corresponding *in* transition structures, more remarkable in the case of the ammonium cation. This exception can be explained in terms of stabilizing electrostatic interactions between the inward substituents and the delocalized aromatic  $\pi$ -system.

The different stereochemical trends observed for [ $_{\tau}8_c$ ] reactions with respect to the corresponding [ $_{\tau}4_c$ ] electrocyclizations can be understood taking into account the important differences between the transition structures involved in both processes, despite their similar orbital topologies. Thus, in the transition structures associated with [ $_{\tau}4_c$ ] reactions, there is a considerable torsion about the terminal C–C bonds, with an appreciable  $\phi$  angle between the p AOs of terminal atoms and the line that connects them, associated with formation of the new  $\sigma$  bond (Figure 6A). According to torquoelectronic theory,<sup>4</sup> this torsion generates a high overlap between the AOs of the inward substituent and of the adjacent atom associated with the new  $\sigma$  bond (Figure 6A). This results



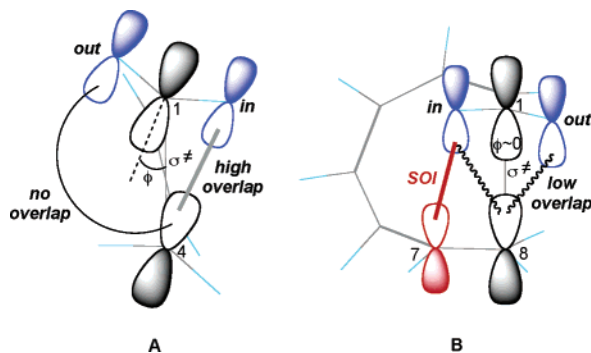


**FIGURE 6.** Stereoelectronic effects in four-electron (A) and eight-electron (B) conrotatory electrocyclic reactions. The AOs leading to the new  $\sigma$  bond are represented in black. The AOs of the substituents and that of the C7 position are represented in blue and red, respectively. In the case of the transition structure associated with the  $[_7,8_c]$  reaction, the secondary orbital interaction (SOI) between the inward substituent and the C7 atom is shown.

in the known preference for inward electrocyclizations when electron acceptors are involved. In contrast, as Houk et al. observed,<sup>7</sup> in the case of  $[_7,8_c]$  reactions the helical geometry of the transition structures generates a low or negligible torsion, with a value for the  $\phi$  angle close to zero (Figure 6B). As a consequence, as far as torquoelectronic effects are concerned, there is no significant difference between the inward and outward positions, since in both cases the overlap between the AOs of the substituents and the p AO of the adjacent atom involved in formation of the new  $\sigma$  bond is low (Figure 6B). This should result in a general preference for the outward orientation regardless of the electron-donating or -accepting character of the substituents, since torquoelectronic effects are not relevant in the eight-electron case.

However, there is another possible stereoelectronic effect in  $[_7,8_c]$  reactions that involves interaction between the inward substituent and the atom contiguous to one of the termini, denoted as C7 in Figure 6B. As we have previously noted, this interaction is favored by the eclipsing between the involved atoms, which results in high overlap between the corresponding AOs. Since this effect does not involve the  $\sigma^*$  localized orbital but the AOs of two atoms not associated with formation of new  $\sigma$  bonds, it corresponds to a secondary orbital interaction (SOI), whose magnitude depends on the donating or accepting character of the substituents and the polyene scaffold. Thus, in *in-TSc* there is a stabilizing interaction between one lone pair of the inward chlorine and the localized  $\pi_{C7,C8}^*$  orbital, as is shown in Figure 7. Therefore, and in contrast with that predicted for four-electron conrotations, a  $\pi$ -donor group can be partially stabilized when it occupies the inward position because of a stabilizing SOI. This should result in lower  $\Delta E_{in-out}$  energy differences, as is shown in Table 2. In addition, a strong acceptor such as formyl can benefit from the reverse SOI. Thus, the NBA of *in-TSk* shows a stabilizing interaction between the  $\pi_{C7,C8}$  and the  $\pi_{C9,O}^*$  localized orbitals (Figure 7). A functional group of intermediate  $\sigma_R^0$  value such as the cyano group can behave as both a

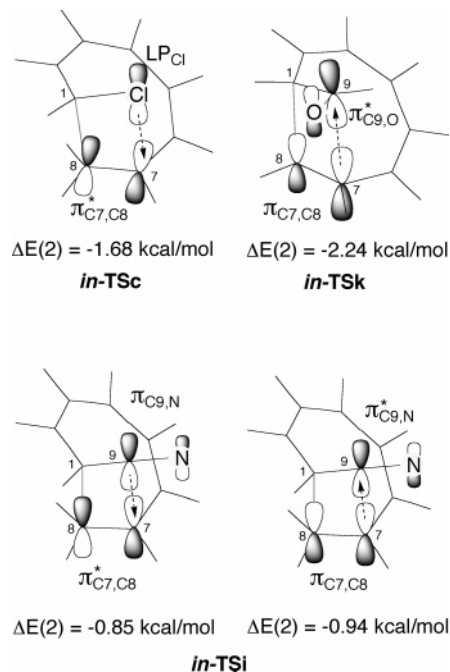


**FIGURE 7.** Main B3LYP/6-31G\* second-order perturbational energies ( $\Delta E(2)$ ) calculated for transition structures *in-TSc*, *in-TSk*, and *in-TSi*, according to the Natural Population Analysis.

$\pi$ -donor and a  $\pi$ -acceptor, as can be seen from the corresponding  $\Delta E(2)$  values reported in Figure 7 for *in-TSi*.

## Conclusions

From the computational studies reported in this paper, the following conclusions can be drawn: (i) The eight-electron conrotatory electrocyclic reaction of octa-1,3,5,7-tetraenes takes place with complete periselectivity via Möbius aromatic transition structures of helical conformation. These transition structures are earlier than their four-electron analogues. (ii) In general, transition structures having outward substituents are preferred with respect to the inward transition structures, irrespective of the  $\pi$ -donor or  $\pi$ -acceptor character of the substituent. (iii) In contrast with four-electron thermal conrotatory electrocyclic reactions, torquoelectronic effects are not relevant, the stereochemical outcome being the result of secondary orbital interactions, electrostatic interactions, and steric effects.

**Acknowledgment.** We thank the Ministerio de Educación y Ciencia of Spain (Projects BQU2001-0904 and CTQ2004-06816/BQU) and the Gobierno Vasco-Eusko Jaurlaritza (Grant 9/UPV 00170.215-13548/2001) for financial support.

**Supporting Information Available:** Figures S1 and S2 showing the geometric features of *in-* and *out-TSb-I* and Cartesian coordinates and energies (including zero-point vibrational energies) of all the reactants, products and transition structures discussed in this work. This material is available free of charge via the Internet at <http://pubs.acs.org>.

JO048874H